A Petrov-Galerkin Multiscale Hybrid-Mixed Method for the Darcy Equation on Polytopes

Honório Fernando, Larissa Martins, Weslley da Silva Pereira, Frédéric Valentin

A Petrov-Galerkin Multiscale Hybrid-Mixed Method for the Darcy Equation on Polytopes

Honório Fernando, Larissa Martins, Weslley Pereira, Frédéric Valentin

October 18, 2022

Abstract

In this work, we propose a new method called Petrov-Galerkin Multiscale Hybrid-Mixed (PGMHM for short) as a variant of the Multiscale Hybrid-Mixed (MHM) method. Its construction starts from a Petrov-Galerkin formulation for the Lagrange multiplier space, defined by enriching the trial spaces with residual-based functions on the partition faces. As a result, jump terms are added to the original MHM method, which penalizes the lack of conformity of MHM numerical solutions. As a consequence of space enrichment, the method induces local postprocessing of the numerical solution that incorporates the model's physical aspects and preserves the exact solution's local conservation properties. Numerical experiments validate the theoretical results and verify the accuracy of PGMHM on highly heterogeneous problems.

Keywords: Darcy equation. Petrov-Galerkin formulation. Multiscale. Hybrid-Mixed Method.

1 Introduction

Multiscale finite element methods have undergone intense development in the last decades, both in theoretical and practical aspects, for their capacity to be accurate on coarse meshes and to be prompt to leverage the new generation of massively parallel computers. Since the seminal work [1], there has been vast literature on the subject wherein the Multiscale Hybrid-Mixed (MHM for short) method [2, 3] is an example. The MHM method is a byproduct of a hybrid formulation that starts at the continuous level posed on a coarse partition. It consists of decomposing the exact solution into local and global contributions. When discretized, such a characterization decouples local and global problems: the global formulation turns out to be responsible for the degrees of freedom over the skeleton of the coarse partition, and the local problems provide the multiscale basis functions. It is interesting that the multiscale basis functions can be computed locally through independent problems. Other alternative multiscale methods share the similarity of a global problem constructed over the solution of local problems that play the role of upscaling the under-mesh structures. In the context of the Darcy model (or Poisson equation), it is worth mentioning the VMS method [4], MsFEM and GMsFEM [5], the PGEM and GEM [6], the HMM [7], Multiscale Mortar method [8], the LOD method [9] and other variants of the MHM method as [10], to cite a few.

The MHM method for the Darcy equation is non-conforming in the H^1 topology as its solution is discontinuous across faces. Finite-dimensional Lagrange multipliers on the skeleton of a partition and element-wise piecewise polynomial drive the approximate solution. Then, we improve the MHM's accuracy by enhancing the finite-dimensional Lagrange multiplier space with functions that enforce the H^1-conformity of the MHM method. Such an idea produces the Petrov-Galerkin Multiscale Hybrid-Mixed method (PGMHM) as a perturbation of the MHM method. Its construction follows the original idea of the Petrov-Galerkin enriched methods (PGEM) [11, 6], which consists of enhancing the trial Lagrange multiplier space and look for a discrete solution in the underlying augmented space through the standard Petrov-Galerkin method. Moreover, this immediately yields a post-processed solution computed from local problems driven by a "more physical" Lagrange multiplier space.

In this work, the enhanced space relies on the a posteriori error estimator proposed in [3, 12]. The proposed approach allows static condensation, which results in adding jump terms associated with the discrete solution to the original MHM method. Those extra terms penalize the lack of H^1-conformity of the MHM solutions. Consequently, the underlying linear system associated with the PGMHM method is no longer of saddle-point type. Also, it permits bridging the proposed multiscale approach with stabilized

methods where the stabilized parameter arises from the design of the a posteriori error estimator. We prove the well-posedness and optimal convergence properties of the new method by taking into account the interplay between the first and second levels of discretization. Numerical validation verifies theoretical findings and also shows that the PGMHM method is super-convergent in some scenarios and can improve the MHM's solution in heterogeneous coefficient problems.

The outline of this manuscript is the following: Notation and some preliminary results are in Section 2. In particular, we recall the characterization of the exact solution in terms of local and global problems. Section 3 introduces the method and present its construction. Existence and unicity for the PGMHM method are proved in Section 4, and error estimates are in Section 5. Numerics are in Section 6 and conclusions are laid in Section 7.

2 Setting and Preliminary Results

2.1 The Darcy model

Let $\Omega \subset \mathbb{R}^d$, $d \in \{2, 3\}$, be an open and bounded domain with polygonal Lipschitz boundary $\partial\Omega$. Given $f \in L^2(\Omega)$ and $g \in H^{\frac{1}{2}}(\partial\Omega)$, this work aims at approximating the following boundary value problem: Find $u \in H^1(\Omega)$ such that $u|_{\partial\Omega} = g$ and

$$\int_\Omega A\nabla u \cdot \nabla v = \int_\Omega f\, v \quad \text{for all } v \in H^1_0(\Omega)\,. \tag{1}$$

Here, $A \in L^\infty(\Omega)^{d\times d}$ is a symmetric matrix and may involve *multiscale* features. It is supposed to be uniformly elliptic in Ω. More precisely, we assume that there exist positive constants $A_{\min}$ and $A_{\max}$ such that

$$A_{\min}|\boldsymbol{\xi}|^2 \le \boldsymbol{\xi}^T A(\boldsymbol{x})\boldsymbol{\xi} \le A_{\max}|\boldsymbol{\xi}|^2 \quad \text{for all } \boldsymbol{\xi} \in \mathbb{R}^d\,, \tag{2}$$

and for almost all $\boldsymbol{x} \in \Omega$, where $|\cdot|$ is the Euclidian norm. The standard weak formulation (1) is a well-posed problem (c.f. [13, Proposition 3.4]).

Above and hereafter, $H^m(D)$ ($L^2(D) = H^0(D)$) stands for the usual Sobolev spaces on an open bounded set $D \subset \mathbb{R}^d$, $d \in \{1, 2, 3\}$.

2.2 Hybrization

Following closely the presentation in [14], we start introducing $\mathscr{P}$, a collection of open, bounded, disjoint polytopes, K, such that $\bar\Omega = \cup_{K\in\mathscr{P}}\bar K$. The shapes of the polytopes K are, a priori, arbitrary, but we suppose that they satisfy a minimal angle condition (see Assumption A, Section 5, for a more precise statement). The diameter of K is $\mathcal{H}_K$ and we denote $\mathcal{H} = \max_{K\in\mathscr{P}}\mathcal{H}_K$, and assume $\mathcal{H} \le 1$. For each $K \in \mathscr{P}$, $\boldsymbol{n}^K$ denotes the unit outward normal to ∂K, such that $\boldsymbol{n}^K = \boldsymbol{n}$ on $\partial\Omega$ where $\boldsymbol{n}$ is the unit outward normal to $\partial\Omega$. We also introduce $\partial\mathscr{P}$ as the set of boundaries ∂K, and $\mathcal{E}$ the set of the faces of $\mathscr{P}$, and $\mathcal{E}_0$ the set of internal faces. By $\boldsymbol{n}_E$ we denote a unit normal vector on faces $E \in \mathcal{E}$, and $\boldsymbol{n}_E^K$ the unit outward normal vector on E with respect to K.

Associated to the partition $\mathscr{P}$, we define the broken Sobolev space $H^m(\mathscr{P}) := \{v : v|_K \in H^m(K) \quad \text{for all } K \in \mathscr{P}\}$, for $m \ge 1$.

In addition, the following spaces will be useful in what follows

$$V := H^1(\mathscr{P}) \quad \text{with norm} \quad \|v\|_V := \left\{\sum_{K\in\mathscr{P}}\left(\frac{1}{d_\Omega^2}\|v\|^2_{0,K} + \|\nabla v\|^2_{0,K}\right)\right\}^{\frac{1}{2}}\,, \tag{3}$$

where $d_\Omega > 0$ is the diameter of Ω, and the space $H^{\frac{1}{2}}(\partial\Omega)$ defined as the trace of functions in $H^1(\Omega)$ equipped with the norm

$$\|g\|_{1/2,\partial\Omega} := \inf_{\substack{v\in H^1(\Omega)\\ v=g \text{ on } \partial\Omega}} \|v\|_V\,. \tag{4}$$

We define

$$V_0 := \{v \in L^2(\Omega) : v|_K \in \mathbb{P}_0(K) \quad \text{for all } K \in \mathscr{P}\}\,, \tag{5}$$

where $\mathbb{P}_0(K)$ stands for the space of piecewise constants, and

$$\tilde V := \{v \in V : v|_K \in L^2_0(K) \quad \text{for all } K \in \mathscr{P}\}\,, \tag{6}$$

where $L^2_0(K)$ is the space function $L^2(K)$ with zero mean value functions. In addition, we define

$$\Lambda := \{\boldsymbol{\tau}\cdot\boldsymbol{n}^K|_{\partial K} \,:\, \boldsymbol{\tau}\in H(\mathrm{div},\Omega) \quad \text{for all } K\in\mathscr{P}\}\,, \tag{7}$$

equipped with the following norm

$$\|\mu\|_\Lambda := \sup_{v\in V}\frac{\langle\mu,v\rangle_{\partial\mathscr{P}}}{\|v\|_V} \quad \text{for all } \mu\in\Lambda\,. \tag{8}$$

We also define the following (semi) norm in Λ

$$|\mu|_\Lambda := \sup_{\tilde{v}\in\tilde{V}}\frac{\langle\mu,\tilde{v}\rangle_{\partial\mathscr{P}}}{\|\tilde{v}\|_V} \quad \text{for all } \mu\in\Lambda\,. \tag{9}$$

Above and hereafter, we lighten notation and understand the supremum to be taken over sets excluding the zero function, even though this is not specifically indicated.

We also denote by $(\cdot,\cdot)_D$ the $L^2(D)$-inner product (we do not make a distinction between vector-valued and scalar-valued functions), and define the products on $\mathscr{P}$ and $\partial\mathscr{P}$ as

$$(v,w)_{\mathscr{P}} := \sum_{K\in\mathscr{P}}(v,w)_K \quad \text{and} \quad \langle\mu,v\rangle_{\partial\mathscr{P}} := \sum_{K\in\mathscr{P}}\langle\mu,v\rangle_{\partial K}\,, \tag{10}$$

where the product on ∂D is the duality pairing between $H^{-\frac{1}{2}}(\partial D)$ and $H^{\frac{1}{2}}(\partial D)$. Also, we shall use the following space product norm in $\Lambda\times V$

$$\|(\mu,v)\|_{\Lambda\times V} := \|\mu\|_\Lambda + \|v\|_V\,. \tag{11}$$

We are ready to present a hybrid formulation for (1). Here, we relax continuity of u on the skeleton $\partial\mathscr{P}$ by introducing the Lagrange multiplier λ. The hybrid formulation reads: Find $(\lambda,u)\in\Lambda\times V$ such that

$$\begin{cases} (A\nabla u,\nabla v)_{\mathscr{P}} - \langle\lambda,v\rangle_{\partial\mathscr{P}} = (f,v)_{\mathscr{P}} & \text{for all } v\in V,\\ \langle\mu,u\rangle_{\partial\mathscr{P}} = \langle\mu,g\rangle_{\partial\Omega} & \text{for all } \mu\in\Lambda. \end{cases} \tag{12}$$

Observe that (12) is a saddle point problem wherein the exact solution u is searched in a space V bigger than $H^1(\Omega)$. Nonetheless, the introduction of the Lagrange multiplier $\lambda\in\Lambda$, which ensures the weak continuity of u on $\mathscr{P}$, leads u to belong to $H^1(\Omega)$ and to satisfy the original formulation (1). These results were proved in [15] and extended in [16] to more general partitions $\mathscr{P}$.

2.3 A characterization of the exact solution

The exact solution can be characterized in terms of the solution of local and global problems. Following closely [3], we define the bounded mappings $T\in\mathcal{L}(\Lambda,V)$ and $\hat{T}\in\mathcal{L}(L^2(\Omega),V)$ as follows

- for all $\mu\in\Lambda$, $T\mu\,|_K\in H^1(K)\cap L^2_0(K)$ is the unique solution of

$$\int_K A\nabla T\mu\cdot\nabla v = \langle\mu,v\rangle_{\partial K} \quad \text{for all } v\in H^1(K)\cap L^2_0(K)\,,\ \forall\, K\in\mathscr{P}\,; \tag{13}$$

- for all $q\in L^2(\Omega)$, $\hat{T}q\,|_K\in H^1(K)\cap L^2_0(K)$ is the unique solution of

$$\int_K A\nabla\hat{T}q\cdot\nabla v = \int_K q\,v \quad \text{for all } v\in H^1(K)\cap L^2_0(K)\,,\ \forall\, K\in\mathscr{P}\,. \tag{14}$$

Hence, the solution of (1) can be written

$$u = u_0 + T\lambda + \hat{T}f\,, \tag{15}$$

where $(\lambda,u_0)\in\Lambda\times V_0$ solve the following mixed problem: Find $(\lambda,u_0)\in\Lambda\times V_0$ such that

$$\begin{cases} \langle\mu,T\lambda\rangle_{\partial\mathscr{P}} + \langle\mu,u_0\rangle_{\partial\mathscr{P}} = -\langle\mu,\hat{T}f\rangle_{\partial\mathscr{P}} + \langle\mu,g\rangle_{\partial\Omega} & \text{for all } \mu\in\Lambda\,,\\ \langle\lambda,v_0\rangle_{\partial\mathscr{P}} = -(f,v_0)_{\mathscr{P}} & \text{for all } v_0\in V_0\,. \end{cases} \tag{16}$$

The well-posedness of (16) was proved in [3] and is stated below for the sake of completeness.

Theorem 2.1. *There exist positive constants C such that*

$$\langle \mu, T\mu \rangle_{\partial\mathscr{P}} \geq C \, \|\mu\|_{\Lambda}^2 \quad \textit{for all } \mu \in \mathscr{N} \,, \tag{17}$$

$$\sup_{\mu \in \Lambda} \frac{\langle \mu, v_0 \rangle_{\partial\mathscr{P}}}{\|\mu\|_{\Lambda}} \geq C \, \|v_0\|_V \quad \textit{for all } v_0 \in V_0 \,, \tag{18}$$

where

$$\mathscr{N} := \{ \mu \in \Lambda \,:\, \langle \mu, v_0 \rangle_{\partial\mathscr{P}} = 0 \quad \textit{for all } v_0 \in V_0 \} \,. \tag{19}$$

Consequently, (16) has a unique solution $(\lambda, u_0) \in \Lambda \times V_0$. Moreover, u given in (15) satisfies (1) and $A\nabla u \cdot \boldsymbol{n}^K \,|_{\partial K} = \lambda$ for all $K \in \mathscr{P}$.

Proof. See [3, Section 3.1] for the partition of Ω in simplex elements, and [14, Theorem 2.1] for more general cases. □

Observe that (9) is a norm on the null space $\mathscr{N}$ as it coincides with $\|\cdot\|_{\Lambda}$. Also, $\boldsymbol{\sigma} := A\nabla u \in H(\mathrm{div}, \Omega)$ since $\boldsymbol{\sigma} \cdot \boldsymbol{n}^K \,|_{\partial K} \in \Lambda$ for all $K \in \mathscr{P}$. In addition, since $T\lambda$ and $\hat{T}f$ have zero mean value in every $K \in \mathscr{P}$ the following holds

$$u_0|_K = \frac{1}{|K|} \int_K u \,.$$

3 The PGMHM method

3.1 Partitions and finite dimensional broken spaces

Similar to the MHM method (c.f. [17, Section 3]), the PGMHM uses a multi-level discretization starting from the first level partition $\mathscr{P}$. We introduce two partitions which do not coincide but are not independent. We start discretizing the set of faces $E \in \mathcal{E}$ and denote by $\mathcal{H}_E$ its diameter. For this, we introduce $\mathcal{E}_H$, a partition of $\mathcal{E}$, for which each $E \in \mathcal{E}$ is split into faces F of diameter $H_F \leq H := \max_{F \in \mathcal{E}_H} H_F$. Hereafter, we shall assume the existence of C, independent of mesh sizes, such that

$$\mathcal{H}_K \leq C \, \mathcal{H}_E \quad \text{for all } E \subset \mathcal{E} \text{ and } K \in \mathscr{P} \,. \tag{20}$$

In addition, for each $K \in \mathscr{P}$, we introduce a shape regular family of simplicial triangulations $\{\mathscr{T}_h^K\}_{h>0}$ made up of simplices $T \in \mathscr{T}_h^K$ of diameter $h_T \leq h := \max_{K \in \mathscr{P}} \max_{T \in \mathscr{T}_h^K} h_T$ (see Figure 1). Also, we restrict $\mathcal{E}_H$ to be simplicial and shape regular in order to avoid unnecessary technicalities in the presentation of the method and the proofs.

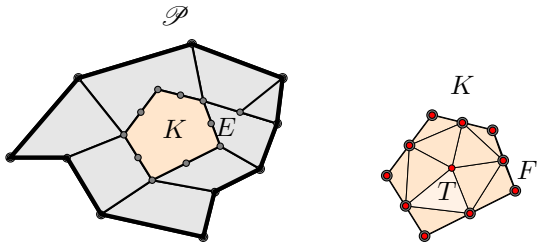

Figure 1: A polytopal domain discretized with non-conforming polygonal elements K (left) and a minimal sub-mesh in element K (right). The red dots represent the degrees of freedom associated with the sub-mesh and the gray dots with the mesh skeleton.

The term $[\![v]\!]$ represents the jump of v on $E \in \mathcal{E}$, i.e., for two elements K and K' sharing E, we define

$$[\![v]\!] := (\boldsymbol{n}_E^K \cdot \boldsymbol{n}_E) v \,|_K + (\boldsymbol{n}_E^{K'} \cdot \boldsymbol{n}_E) v \,|_{K'} \quad \text{on } E \in \mathcal{E}_0 \,,$$

and $[\![v]\!] = v$ on $E \subset \partial\Omega$. We define finite element spaces associated to $\mathcal{E}_H$ and $\mathscr{T}_h^K$ given as follows

$$V_h := \prod_{K\in\mathscr{P}} V_h(K) \;\text{ where }\; V_h(K) := \{v_h \in C^0(K) : v_h|_T \in \mathbb{P}_k(T),\, \forall\, T \in \mathscr{T}_h^K\}\,, \tag{21}$$

$$\tilde{V}_h := \prod_{K\in\mathscr{P}} \tilde{V}_h(K) \;\text{ where }\; \tilde{V}_h(K) := V_h(K) \cap L^2_0(K)\,, \tag{22}$$

$$\Lambda_H := \{\mu_H \in \Lambda : \mu_H|_F \in \mathbb{P}_\ell(F),\, \forall\, F \in \mathcal{E}_H\} \quad \text{with } k \geq \ell + d\,,\, \ell \geq 0. \tag{23}$$

Here $\mathbb{P}_m(D)$ stands for the space of polynomials with degree of order less or equal to $m \geq 0$. Using the finite element spaces defined in (21)-(22), the discrete equivalents of the mappings T and $\hat{T}$ defined in (13)-(14) read

- for all $\mu \in \Lambda$, $T_h\mu \in \tilde{V}_h$ is the unique solution of

$$\int_K A\nabla T_h\mu \cdot \nabla v_h \;= \langle \mu, v_h\rangle_{\partial K} \quad \text{for all } v_h \in \tilde{V}_h(K) \quad \text{and} \quad K \in \mathscr{P}\,; \tag{24}$$

- for all $q \in L^2(\Omega)$, $\hat{T}_h q \in \tilde{V}_h$ is the unique solution of

$$\int_K A\nabla \hat{T}_h q \cdot \nabla v_h \;= \int_K q\, v_h \quad \text{for all } v_h \in \tilde{V}_h(K) \quad \text{and} \quad K \in \mathscr{P}\,. \tag{25}$$

Following [14], for $\mu \in \Lambda$ and $q \in L^2(\Omega)$ the following stability results hold

$$\|T_h\mu\|_V \;\leq\; \frac{C}{A_{\min}}\,|\mu|_\Lambda \quad \text{and} \quad \|\hat{T}_h q\|_V \;\leq\; \frac{C}{A_{\min}}\,\mathcal{H}\,\|q\|_{0,\Omega}\,, \tag{26}$$

where C depends only on the constant in the Poincaré inequality (c.f. [17, §2.4]). Hereafter, we denote by C a positive constant independent of mesh sizes, which may dependent of physical coefficients $A_{\min}$ and $A_{\max}$. The constant dependency on the shape of mesh elements follows [17, Remark 2.1],

3.2 The method

We propose to approximate the solution of (16) by the following PGMHM method: Find $(\lambda_H, u_0^h) \in \Lambda_H \times V_0$ such that

$$\begin{cases} a_h(\lambda_H, \mu_H) + b_h(\mu_H, u_0^h) = \hat{f}_h(\mu_H) + g_h(\mu_H)\,, \\ b_h(\lambda_H, v_0) + c_h(u_0^h, v_0) = f_h(v_0) + \hat{g}_h(v_0)\,, \end{cases} \tag{27}$$

for all $(\mu_H, v_0) \in \Lambda_H \times V_0$. The discrete bilinear forms above rely on the mappings (24)-(25), and read

$$\begin{cases} a_h : \Lambda\times\Lambda \to \mathbb{R} & a_h(\lambda_H,\mu_H) = \langle \mu_H, T_h\lambda_H\rangle_{\partial\mathscr{P}} + \displaystyle\sum_{E\in\mathcal{E}} \tau_E\,([\![T_h\,\mu_H]\!], [\![T_h\,\lambda_H]\!])_E\,, \\ b_h : \Lambda\times V_0 \to \mathbb{R} & b_h(\lambda_H, v_0) = \langle \lambda_H, v_0\rangle_{\partial\mathscr{P}} + \displaystyle\sum_{E\in\mathcal{E}} \tau_E\,([\![T_h\,\lambda_H]\!], [\![v_0]\!])_E\,, \\ c_h : V_0\times V_0 \to \mathbb{R} & c_h(u_0^h, v_0) = \displaystyle\sum_{E\in\mathcal{E}} \tau_E\,(\left[\!\left[u_0^h\right]\!\right], [\![v_0]\!])_E\,, \end{cases} \tag{28}$$

and the discrete linear forms

$$\begin{cases} f_h : V_0 \to \mathbb{R} & f_h(v_0) = -(f, v_0)_{\mathscr{P}} - \displaystyle\sum_{E\in\mathcal{E}} \tau_E\,(\left[\!\left[\hat{T}_h\, f\right]\!\right], [\![v_0]\!])_E\,, \\ \hat{f}_h : \Lambda \to \mathbb{R} & \hat{f}_h(\mu_H) = -\langle \mu_H, \hat{T}_h f\rangle_{\partial\mathscr{P}} - \displaystyle\sum_{E\in\mathcal{E}} \tau_E\,([\![T_h\,\mu_H]\!], \left[\!\left[\hat{T}_h\, f\right]\!\right])_E\,, \\ g_h : \Lambda \to \mathbb{R} & g_h(\mu_H) = \langle \mu_H, g\rangle_{\partial\Omega} + \displaystyle\sum_{E\subset\partial\Omega} \tau_E\,(T_h\mu_H, g)_E\,, \\ \hat{g}_h : V_0 \to \mathbb{R} & \hat{g}_h(v_0) = \displaystyle\sum_{E\subset\partial\Omega} \tau_E\,(g, v_0)_E\,. \end{cases} \tag{29}$$

Here, the mesh-dependent parameter τ_E reads

$$\tau_E := \frac{\alpha\, A_{min}}{2\,\mathcal{H}_E} \quad \text{where} \quad \alpha \in \mathbb{R}^+ \;\text{ in } \Omega\,. \tag{30}$$

Next, following the MHM methodology described in [3], a discrete solution u_{Hh} can be reconstructed from the solution of (27) as follows

$$u_{Hh} := u_0^h + T_h \lambda_H + \hat{T}_h f . \tag{31}$$

In the present framework, an alternative discrete solution $\tilde{u}_{Hh}$ is available driven by a richer subspace of Λ. This option stems from an enriching space approach and shall become clear in the next section. For now, let us define $\lambda_R \in \Lambda$ such that

$$\lambda_R|_E := \begin{cases} \pm \tau_E \, [\![u_{Hh}]\!] \, |_E & \text{if } E \in \mathcal{E}_0 , \\ \pm \tau_E \, (u_{Hh} - \pi_k \, g) \, |_E & \text{if } E \subset \partial\Omega , \end{cases} \tag{32}$$

where π_k is the $L^2(E)$ orthogonal projection on $\mathbb{P}_k(E)$ and $\pm$ represents the sign of $\boldsymbol{n}_E \cdot \boldsymbol{n}_E^K$. Observe that $\lambda_R|_E \in \mathbb{P}_k(E)$, and then, $\lambda_R \notin \Lambda_H$. Then, we define $u_R := T_h \lambda_R \in \tilde{V}_h$ such that, when restricted to $K \in \mathscr{P}$, it satisfies

$$\int_K A \nabla T_h \lambda_R \cdot \nabla v_h = \langle \lambda_R, v_h \rangle_{\partial K} \quad \text{for all } v_h \in \tilde{V}_h(K) . \tag{33}$$

Thereby, we propose to approximate the exact solution by

$$\tilde{u}_{Hh} := u_{Hh} + u_R = u_0^h + T_h \tilde{\lambda}_H + \hat{T}_h f \quad \text{where} \quad \tilde{\lambda}_H := \lambda_H + \lambda_R . \tag{34}$$

Remark 3.1. At this point, observe that the local conservative property of the exact flux λ is preserved by its discrete counterpart $\tilde{\lambda}_H$, but not by λ_H. Indeed, replacing $(v_0, \lambda_H) = (1_K, 0)$ in the second equation in (27), it holds

$$\int_{\partial K} \tilde{\lambda}_H = \int_{\partial K} \left(\lambda_H + \lambda_R \right) = - \int_K f \quad \text{for all } K \in \mathscr{P} ,$$

where λ_R is given in (32). The choice of a numerical method to define T_h and $\hat{T}_h$ can be general. Here, we restrict the presentation and analysis to a Galerkin method, but other choices, such as stabilized or enriched methods, or discontinuous Galerkin related methods, to name a few, are also options which lead to similar theoretical results. Error estimates for both discrete solutions u_{Hh} and $\tilde{u}_{Hh}$ will be addressed in Section 5.

3.3 Derivation of the method

In this section, we present an interpretation of the PGMHM method as a byproduct of an enriching space strategy, which leads to the post-processed discrete solution $\tilde{u}_{Hh}$ in (34). Indeed, we adapt the enriching space framework based on a posteriori error estimators originally proposed in [18] to hybrid formulation. As a result, we augment the space Λ_H with functions dependent on the jumps of the discrete solution on faces.

We formalize such an idea by starting with the following augmented space

$$\tilde{\Lambda}_H := \Lambda_H + \Lambda_R ,$$

where Λ_H is defined in (23) and $\Lambda_R \subset \Lambda$ is given by

$$\Lambda_R := \{ \mu_R \in \Lambda \, : \, \mu_R = [\![w_h]\!] \, |_E \in \mathbb{P}_k(E) \quad \forall w_h \in V_h, \; E \in \mathcal{E} \} .$$

As such, a function $\tilde{\mu}_H \in \tilde{\Lambda}_H$ can be decomposed (not uniquely) as follows

$$\tilde{\mu}_H = \mu_H + \mu_R , \tag{35}$$

where $\mu_H \in \Lambda_H$ and $\mu_R \in \Lambda_R$. In the particular case of $\tilde{\lambda}_H$, we look for λ_R such that it depends on the residual on faces. As a result, its definition involves the jumps of the discrete solution u_{Hh} as shown in the a posteriori estimator proposed in [3].

Specifically, we search $\lambda_R \in \Lambda_R$ as in (32), where $u_{Hh} := u_0^h + T_h \lambda_H + \hat{T}_h f \in V_h$ and τ_E is given in (30). This can be seen as a consistent perturbation (or enrichment) of $\lambda_H \in \Lambda_H$ since λ_R vanishes as u_{Hh} converges to u.

Owing to these definitions, we discretize the hybrid problem (16) using the following *Petrov-Galerkin* strategy: Find $\tilde{\lambda}_H \in \tilde{\Lambda}_H$ and $u_0^h \in V_0$ such that

$$\begin{cases} \langle \mu_H, T_h \tilde{\lambda}_H \rangle_{\partial\mathscr{P}} + \langle \mu_H, u_0^h \rangle_{\partial\mathscr{P}} = -\langle \mu_H, \hat{T}_h f \rangle_{\partial\mathscr{P}} + \langle \mu_H, g \rangle_{\partial\Omega} \quad \text{for all } \mu_H \in \Lambda_H \,, \\ \langle \tilde{\lambda}_H, v_0 \rangle_{\partial\mathscr{P}} = -(f, v_0)_{\mathscr{P}} \quad \text{for all } v_0 \in V_0 \,, \end{cases} \tag{36}$$

and the corresponding enriched numerical approximation writes

$$\tilde{u}_{Hh} := u_0^h + T_h \, \tilde{\lambda}_H + \hat{T}_h \, f \,.$$

Observe that the method (36) is not, apparently, prompt to be used since it depends on the action of T_h on λ_R, which is not available at this point. However, by a simple trick based on the symmetry of operator T_h, we can rewrite (36) in an equivalent form, which we can solve. To see this, first observe that, by symmetry, there holds

$$\langle \mu_H, T_h \lambda_R \rangle_{\partial\mathscr{P}} = \langle \lambda_R, T_h \mu_H \rangle_{\partial\mathscr{P}} \quad \text{for all } \mu_H \in \Lambda_H \,.$$

As a result of the above identity, we get

$$\begin{aligned} &\langle \mu_H, T_h \tilde{\lambda}_H \rangle_{\partial\mathscr{P}} + \langle \mu_H, u_0^h \rangle_{\partial\mathscr{P}} \\ &\quad = \langle \mu_H, T_h \lambda_H \rangle_{\partial\mathscr{P}} + \langle \lambda_R, T_h \mu_H \rangle_{\partial\mathscr{P}} + \langle \mu_H, u_0^h \rangle_{\partial\mathscr{P}} \\ &\quad = \langle \mu_H, T_h \lambda_H \rangle_{\partial\mathscr{P}} + \sum_{E \in \mathcal{E}_0} \tau_E \left([\![T_h \mu_H]\!], [\![u_{Hh}]\!] \right)_E + \sum_{E \subset \partial\Omega} \tau_E (T_h \mu_H, u_{Hh})_E \\ &\quad - \sum_{E \subset \partial\Omega} \tau_E \left(T_h \mu_H, g \right)_E + \langle \mu_H, u_0^h \rangle_{\partial\mathscr{P}} \\ &\quad = a_h(\lambda_H, \mu_H) + b_h(\mu_H, u_0^h) + \sum_{E \in \mathcal{E}} \tau_E \left([\![T_h \mu_H]\!], \left[\!\left[\hat{T}_h f \right]\!\right] \right)_E - \sum_{E \subset \partial\Omega} \tau_E \left(T_h \mu_H, g \right)_E \,, \end{aligned}$$

and

$$\begin{aligned} \langle \tilde{\lambda}_H, v_0 \rangle_{\partial\mathscr{P}} &= \langle \lambda_H, v_0 \rangle_{\partial\mathscr{P}} + \sum_{E \in \mathcal{E}_0} \tau_E \left([\![u_{Hh}]\!], [\![v_0]\!] \right)_E \\ &\quad + \sum_{E \subset \partial\Omega} \tau_E (u_{Hh}, v_0)_E - \sum_{E \subset \partial\Omega} \tau_E (g, v_0)_E \\ &= b_h(\lambda_H, v_0) + c_h(u_0^h, v_0) + \sum_{E \in \mathcal{E}} \tau_E \left(\left[\!\left[\hat{T}_h f \right]\!\right], [\![v_0]\!] \right)_E - \sum_{E \subset \partial\Omega} \tau_E (g, v_0)_E \,. \end{aligned}$$

The PGMHM method (27) follows collecting the previous contributions.

4 Well-posedness

First, we introduce some mesh-dependent norms in V and recall some classical inequalities needed in the proofs. Let

$$\|v\|_{\mathcal{H}} := \left\{ \|\nabla v\|_{0,\mathscr{P}}^2 + \sum_{E \in \mathcal{E}} \frac{1}{\mathcal{H}_E} \|[\![v]\!]\|_{0,E}^2 \right\}^{1/2} , \tag{37}$$

and the product norm

$$\|(\mu, v)\|_{\Lambda \times \mathcal{H}} := \|\mu\|_{\Lambda} + \|v\|_{\mathcal{H}} \,. \tag{38}$$

We also define the product (semi) norm

$$|(\mu, v)|_{\Lambda \times \mathcal{H}} := |\mu|_{\Lambda} + \|v\|_{\mathcal{H}} \,, \tag{39}$$

and observe that (39) is a norm on the polynomial space Λ_H (and $\tilde{\Lambda}_H$) and coincides with the norm $\|\cdot\|_{\Lambda \times \mathcal{H}}$ on the null space $\mathscr{N}$.

Using **[bre03]** and the definition of $\|\cdot\|_{\mathcal{H}}$ in (37) and $\|\cdot\|_V$ in (3), where C is a positive constant that depends only on the shape regularity of the partition $\mathscr{P}$, it holds

$$\|v\|_V \;\leq\; C\,\|v\|_{\mathcal{H}}\,. \tag{40}$$

Also, from the trace inequality in [19, Lemma 6.4] and (20), we have

$$\sum_{E\in\mathcal{E}}\frac{1}{\mathcal{H}_E}\|[\![v]\!]\|_{0,E}^2 \;\leq\; C\sum_{K\in\mathscr{P}}\Big(\frac{1}{\mathcal{H}_K^2}\|v\|_{0,K}^2+\|\nabla v\|_{0,K}^2\Big)\,, \tag{41}$$

and if $v\in\tilde{V}$, from the generalized Poincaré inequality (c.f. [20, 21])), it holds

$$\|v\|_{0,K} \;\leq\; C\,\mathcal{H}_K\|\nabla v\|_{0,K}\,.$$

By replacing the inequality above in (41), one gets

$$\sum_{E\in\mathcal{E}}\frac{1}{\mathcal{H}_E}\|[\![v]\!]\|_{0,E}^2 \;\leq\; C\sum_{K\in\mathscr{P}}\|\nabla v\|_{0,K}^2 \;\leq\; C\,\|v\|_V^2\,, \tag{42}$$

for $v\in H^1(K)\cap L_0^2(K)$. We recall that all the results presented below were proved using constants depending on the shape of the elements in $\mathscr{T}_h^K$. So, although the constants do not depend explicitly on the shape of K, they will depend on an implicit way through the shape of the elements on $\mathscr{T}_h^K$ (see [17, Remark 2.1]).

Now, let $\mathscr{C}_h : H^1(\Omega)\to V_h$ be a variant of the Clément interpolation operator defined locally. That is, for every $v\in V$, we define $\mathscr{C}_h(v)|_K = \mathscr{C}_h^K(v)$, where $\mathscr{C}_h^K : V(K)\to V_h(K)$ is the usual Clément interpolation operator. This mapping satisfies the following (see [13]): there exists C, depending only on the shape of the elements $T\in\mathscr{T}_h^K$ such that, for all $v\in V(K)$ and all $T\in\mathscr{T}_h^K$,

$$\begin{aligned}
\|\mathscr{C}_h^K(v)\|_{1,T} &\leq C\,\|v\|_{1,\omega_T}\,,\\
\|v-\mathscr{C}_h^K(v)\|_{1,T} &\leq C\,\|v\|_{1,\omega_T}\,,\\
\|v-\mathscr{C}_h^K(v)\|_{0,T} &\leq Ch\,\|v\|_{1,\omega_T}\,,
\end{aligned} \tag{43}$$

where $\omega_T := \{T'\in\mathscr{T}_h^K : T\cap T'\neq\emptyset\}$.

The following result ensures the existence of a Fortin operator acting on V with image in V_h and using the space Λ_H. It is the key to the well-posedness of (27). It was addressed in [14] for the two-dimensional case, where $\ell=k$ and $\ell=k+1$ on polytopal domains, and extended to the two- and three-dimensional case in [22] assuming $k\geq\ell+d$, $\ell\geq 0$. We recall a variant of it here in the scalar case [17, Lemma 4.2].

Lemma 4.1. *Let $k-d\geq\ell\geq 1$. Then, there exists a mapping $\Pi_h : V\to V_h$ such that, for all $v\in V$:*

$$\begin{cases}\displaystyle\int_F\Pi_h(v)\mu_H=\int_F v\,\mu_H \quad \textit{for all } \mu_H\in\Lambda_H \quad \textit{and } F\in\mathcal{E}_H\,,\\ \|\Pi_h(v)\|_V\leq C\,\|v\|_V\,.\end{cases} \tag{44}$$

We are ready to prove the well-posedness of the PGMHM method (27). To this end, let $B_h : [\Lambda\times V_0]\times[\Lambda\times V_0]\to\mathbb{R}$ be the following bilinear form

$$B_h(\mu,v_0;\xi,w_0) := a_h(\mu,\xi)+b_h(\xi,v_0)+b_h(\mu,w_0)+c_h(v_0,w_0)\,, \tag{45}$$

and $F_h : [\Lambda\times V_0]\to\mathbb{R}$ the following linear form

$$F_h(\xi,w_0) := f_h(w_0)+\hat{f}_h(\xi)+g_h(\xi)+\hat{g}_h(w_0)\,. \tag{46}$$

Owing to those definitions, we introduce the following equivalent form of the PGMHM method (27): Find $(\lambda_H,u_0)\in\Lambda_H\times V_0$ such that

$$B_h(\lambda_H,u_0;\mu_H,v_0) \;=\; F_h(\mu_H,v_0) \quad \text{for all } (\mu_H,v_0)\in\Lambda_H\times V_0\,. \tag{47}$$

The next results prove the continuity of operators $B_h(\cdot;\cdot)$ and $F_h(\cdot)$, and estimates the consistency error involving in approximating the second-level solutions.

Theorem 4.2. *The mappings $B_h(\cdot;\cdot)$ and $F_h(\cdot)$ are continuous, i.e., there exist C such that*

$$\begin{aligned} B_h(\mu, v_0; \xi, w_0) &\le C\,\|(\mu, v_0)\|_{\Lambda\times\mathcal{H}}\|(\xi, w_0)\|_{\Lambda\times\mathcal{H}} \quad \textit{for all } (\mu,\ v_0),\ (\xi, w_0) \in \Lambda \times V_0\,, \\ F_h(\xi, w_0) &\le C\,\|(\xi, w_0)\|_{\Lambda\times\mathcal{H}} \quad \textit{for all } (\xi, w_0) \in \Lambda \times V_0\,. \end{aligned} \tag{48}$$

Moreover, there exists C such that

$$\sup_{(\chi_H, w_0)\in\Lambda_H\times V_0} \frac{B_h(\lambda-\lambda_H, u_0-u_0^h; \chi_H, w_0)}{|(\chi_H, w_0)|_{\Lambda\times\mathcal{H}}} \le C\,\|(T-T_h)\lambda + (\hat{T}-\hat{T}_h)f\|_V\,, \tag{49}$$

where (u_0, λ) is the solution of (16).

Proof. The proof of continuity of forms $B_h(\cdot,\cdot)$ and $F_h(\cdot)$ in (48) follows easily from the definition of norms $\|\cdot\|_V$, $\|\cdot\|_\Lambda$ and $\|\cdot\|_{1/2,\partial\mathscr{P}}$ in (3), (8) and (4), respectively, Cauchy-Schwartz and trace inequality (41), and the stability of operators T_h and $\hat{T}_h$ in (26).

As for the consistency error estimate (49), we split it in two parts using the fact that, from the definition of (45), it holds

$$\begin{aligned} B_h(\lambda-\lambda_H, u_0-u_0^h; \chi_H, w_0) = &\underbrace{a_h(\lambda-\lambda_H, \chi_H) + b_h(\chi_H, u_0-u_0^h)}_{(i)} \\ &+ \underbrace{b_h(\lambda-\lambda_H, w_0) + c_h(u_0-u_0^h, w_0)}_{(ii)}\,. \end{aligned}$$

First, using the characterization of the exact solution u in (15) and the approximate solution u_{Hh} in (31), and observing that $[\![u]\!] = 0$ on $E \in \mathcal{E}_0$ and $u - g = 0$ on $E \subset \partial\Omega$, we get from the definitions of $b_h(\cdot,\cdot)$ and $c_h(\cdot,\cdot)$ in (28), that

$$b_h(\lambda-\lambda_H, w_0) + c_h(u_0-u_0^h, w_0) = \sum_{E\in\mathcal{E}} \tau_E\Big(\Big[\!\Big[(T_h-T)\lambda + (\hat{T}_h-\hat{T})f\Big]\!\Big], [\![w_0]\!]\Big)_E\,.$$

Next, from the Cauchy-Schwarz inequality and applying the trace inequality (42) and (37), we obtain that (ii) can be bounded as follows

$$\begin{aligned} &b_h(\lambda-\lambda_H, w_0) + c_h(u_0-u_0^h, w_0) \\ &\quad\le \sum_{E\in\mathcal{E}} \tau_E \Big\|\Big[\!\Big[(T_h-T)\lambda + (\hat{T}_h-\hat{T})f\Big]\!\Big]\Big\|_{0,E}\|[\![w_0]\!]\|_{0,E} \\ &\quad\le C\,\|(T-T_h)\lambda + (\hat{T}-\hat{T}_h)f\|_V \Big[\sum_{E\in\mathcal{E}} \frac{1}{\mathcal{H}_E}\|[\![w_0]\!]\|_{0,E}^2\Big]^{1/2} \\ &\quad\le C\,\|(T-T_h)\lambda + (\hat{T}-\hat{T}_h)f\|_V \|w_0\|_{\mathcal{H}}\,. \end{aligned}$$

For the second part (i), we use the same arguments as in (ii) and the definitions of $a_h(\cdot,\cdot)$ and $b_h(\cdot,\cdot)$ in (28), to get

$$\begin{aligned} a_h(\lambda-\lambda_H, \chi_H) + b_h(\chi_H, u_0-u_0^h) =& \langle \chi_H, (T_h-T)\lambda + (\hat{T}_h-\hat{T})f\rangle_{\partial\mathscr{P}} \\ &+ \sum_{E\in\mathcal{E}} \tau_E([\![T_h\chi_H]\!], \Big[\!\Big[(T_h-T)\lambda + (\hat{T}_h-\hat{T})f\Big]\!\Big])_E\,, \end{aligned}$$

and, from the Cauchy-Schwartz inequality and applying the trace inequality (42) and (26), we arrive at

$$\begin{aligned} &a_h(\lambda-\lambda_H, \chi_H) + b_h(\chi_H, u_0-u_0^h) \\ &\quad\le \sup_{\tilde{v}\in\tilde{V}} \frac{\langle\chi_H, \tilde{v}\rangle_{\partial\mathscr{P}}}{\|\tilde{v}\|_V}\|(T_h-T)\lambda + (\hat{T}_h-\hat{T})f\|_V \\ &\qquad + \sum_{E\in\mathcal{E}} \tau_E([\![T_h\chi_H]\!], \Big[\!\Big[(T_h-T)\lambda + (\hat{T}_h-\hat{T})f\Big]\!\Big])_E \\ &\quad\le \|(T-T_h)\lambda + (\hat{T}-\hat{T}_h)f\|_V|\chi_H|_\Lambda \\ &\qquad + \sum_{E\in\mathcal{E}} \tau_E \Big\|\Big[\!\Big[(T_h-T)\lambda + (\hat{T}_h-\hat{T})f\Big]\!\Big]\Big\|_{0,E}\|[\![T_h\chi_H]\!]\|_{0,E} \\ &\quad\le C\,\|(T-T_h)\lambda + (\hat{T}-\hat{T}_h)f\|_V|\chi_H|_\Lambda\,. \end{aligned}$$

Therefore, from the definition of $B_h(\cdot,\cdot)$, we get the following estimate

$$\begin{aligned}\sup_{(\chi_H,w_0)\in\Lambda_H\times V_0}&\frac{B_h(\lambda-\lambda_H,u_0-u_0^h;\chi_H,w_0)}{|(\chi_H,w_0)|_{\Lambda\times\mathcal{H}}}\\ &\le C\sup_{(\chi_H,w_0)\in\Lambda_H\times V_0}\frac{\|(T-T_h)\lambda+(\hat{T}-\hat{T}_h)f\|_V(|\chi_H|_\Lambda+\|w_0\|_{\mathcal{H}})}{|(\chi_H,w_0)|_{\Lambda\times\mathcal{H}}}\\ &\le C\,\|(T-T_h)\lambda+(\hat{T}-\hat{T}_h)f\|_V\,.\end{aligned}$$

□

Next, we address the well-posedness of (27) (e.g. (47)).

Theorem 4.3. *Let $k\ge\ell+d$ and $\ell\ge 1$. Let $B_h(\cdot,\cdot)$ be given in (45). Hence, there exists a positive constant α_0, independent of h and H, such that for $0<\alpha\le\alpha_0$, problem (27) (e.g. (47)) is well-posed. Moreover, it holds*

$$\sup_{(\xi_H,w_0)\in\Lambda_H\times V_0}\frac{B_h(\mu_H,v_0;\xi_H,w_0)}{|(\xi_H,w_0)|_{\Lambda\times\mathcal{H}}}\ge C\,|(\mu_H,v_0)|_{\Lambda\times\mathcal{H}}\,,\tag{50}$$

for all $(\mu_H,v_0)\in\Lambda_H\times V_0$, where C is a positive constant independent of $\mathcal{H}$, H and h.

Proof. Let $\mathscr{N}_H$ be the following null space

$$\mathscr{N}_H:=\{\xi_H\in\Lambda_H\,:\,b_h(\xi_H,v_0)=0\quad\text{for all } v_0\in V_0\}\,.\tag{51}$$

Let $\xi_H\in\mathscr{N}_H$ and $\theta_H\in\Lambda_R$ be such that $\theta_H|_{E\subset\partial K}:=(\boldsymbol{n}_E^K\cdot\boldsymbol{n}_E)\tau_E[\![T_h\xi_H]\!]$. Define $\mu_H:=\xi_H+\theta_H\in\tilde{\Lambda}_H$, and note from (51) that μ_H satisfies

$$\langle\mu_H,v_0\rangle_{\partial\mathscr{P}}=0\quad\text{for all } v_0\in V_0\,,\tag{52}$$

and

$$|\xi_H|_\Lambda\le 2\|\mu_H\|_\Lambda\,.\tag{53}$$

Indeed,

$$\begin{aligned}|\xi_H|_\Lambda&\le\|\mu_H\|_\Lambda+|\theta_H|_\Lambda\\ &=\|\mu_H\|_\Lambda+\sup_{\tilde{v}\in\tilde{V}}\frac{\langle\theta_H,\tilde{v}\rangle_{\partial\mathscr{P}}}{\|\tilde{v}\|_V}\\ &\le\|\mu_H\|_\Lambda+\sup_{\tilde{v}\in\tilde{V}}\frac{\left(\sum_{E\in\mathcal{E}}\tau_E\,\|[\![T_h\xi_H]\!]\|_{0,E}^2\right)^{1/2}\left(\sum_{E\in\mathcal{E}}\tau_E\,\|[\![\tilde{v}]\!]\|_{0,E}^2\right)^{1/2}}{\|\tilde{v}\|_V}\\ &\le\|\mu_H\|_\Lambda+\alpha\,C\,A_{\min}\,\|T_h\xi_H\|_V\\ &\le\|\mu_H\|_\Lambda+\alpha\,\frac{C_a}{2}\,|\xi_H|_\Lambda\,,\end{aligned}$$

where C_a depends only on the Poincaré and trace constants. Therefore, (53) follows setting $\alpha\le\frac{1}{C_a}$.

From (52), (8), (42) and Lemma 4.1, there exists C such that

$$\begin{aligned}\|\mu_H\|_\Lambda&=\sup_{\tilde{v}\in\tilde{V}}\frac{\langle\mu_H,\tilde{v}\rangle_{\partial\mathscr{P}}}{\|\tilde{v}\|_V}\\ &\le C\sup_{\tilde{v}\in\tilde{V}}\frac{\langle\mu_H,\Pi_h\tilde{v}\rangle_{\partial\mathscr{P}}}{\|\Pi_h\tilde{v}\|_V}\\ &\le C\sup_{v_h\in V_h}\frac{\langle\mu_H,v_h\rangle_{\partial\mathscr{P}}}{\|v_h\|_V}\\ &\le C\sup_{\tilde{v}_h\in\tilde{V}_h}\frac{\langle\mu_H,\tilde{v}_h\rangle_{\partial\mathscr{P}}}{\|\tilde{v}_h\|_V}\\ &\le C\sup_{\tilde{v}_h\in\tilde{V}_h}\frac{\sum_{K\in\mathscr{P}}\int_K A\nabla T_h\mu_H\cdot\nabla\tilde{v}_h}{\|\tilde{v}_h\|_V}\\ &\le C\sup_{\tilde{v}_h\in\tilde{V}_h}\frac{\sum_{K\in\mathscr{P}}\int_K A\nabla T_h\xi_H\cdot\nabla\tilde{v}_h}{\|\tilde{v}_h\|_V}+\sup_{\tilde{v}_h\in\tilde{V}_h}\frac{\sum_{K\in\mathscr{P}}\int_K A\nabla T_h\theta_H\cdot\nabla\tilde{v}_h}{\|\tilde{v}_h\|_V}\,,\end{aligned}$$

and, thus, from the Cauchy-Schwartz inequality, it holds

$$\begin{aligned}\|\mu_H\|_\Lambda &\leq C\Big(\sum_{K\in\mathscr{P}}\|\nabla T_h\xi_H\|_{0,K}^2+\sum_{K\in\mathscr{P}}\|\nabla T_h\theta_H\|_{0,K}^2\Big)^{1/2}\\ &\leq C\Big(\sum_{K\in\mathscr{P}}\|\nabla T_h\xi_H\|_{0,K}^2+|\theta_H|_\Lambda^2\Big)^{1/2}\\ &= C\left(\sum_{K\in\mathscr{P}}\|\nabla T_h\xi_H\|_{0,K}^2+\left(\sup_{\tilde v\in\tilde V}\frac{\langle\theta_H,\tilde v\rangle_{\partial\mathscr{P}}}{\|\tilde v\|_V}\right)^2\right)^{1/2}\\ &\leq C\Big(\sum_{K\in\mathscr{P}}\|\nabla T_h\xi_H\|_{0,K}^2+\sum_{E\in\mathcal{E}}\tau_E\,\|[\![T_h\xi_H]\!]\|_{0,E}^2\Big)^{1/2}. \end{aligned}\tag{54}$$

Next, we use ξ_H in $a_h(\cdot,\cdot)$, (54) and (53) to get

$$\begin{aligned}a_h(\xi_H,\xi_H)&\geq A_{\min}\sum_{K\in\mathscr{P}}\|\nabla T_h\xi_H\|_{0,K}^2+\sum_{E\in\mathcal{E}}\tau_E\,\|[\![T_h\xi_H]\!]\|_{0,E}^2\\ &\geq C\,\|\mu_H\|_\Lambda^2\geq C\,|\xi_H|_\Lambda^2\,.\end{aligned}\tag{55}$$

Also, for all $v_0\in V_0$, from (37) it holds

$$c_h(v_0,v_0)=\sum_{E\in\mathcal{E}}\tau_E\,\|[\![v_0]\!]\|_{0,E}^2\geq C\,\|v_0\|_{\mathcal{H}}^2\,.\tag{56}$$

Next, given $v_0\in V_0$ take $\bar\mu_H\in\Lambda_H$ such that $\bar\mu_H|_{E\subset\partial K}:=(\boldsymbol{n}_E^K\cdot\boldsymbol{n}_E)\frac{1}{\mathcal{H}_E}[\![v_0]\!]$, then

$$\sum_{K\in\mathscr{P}}\langle\bar\mu_H,v_0\rangle_{\partial K}=\sum_{E\in\mathcal{E}}\frac{1}{\mathcal{H}_E}\,\|[\![v_0]\!]\|_{0,E}^2=\|v_0\|_{\mathcal{H}}^2\,.\tag{57}$$

Observe that

$$|\bar\mu_H|_\Lambda=\sup_{\tilde v\in\tilde V}\frac{\langle\bar\mu_H,\tilde v\rangle_{\partial\mathscr{P}}}{\|\tilde v\|_V}\leq C\Big(\sum_{E\in\mathcal{E}}\frac{1}{\mathcal{H}_E}\|[\![v_0]\!]\|_{0,E}^2\Big)^{1/2}=C\,\|v_0\|_{\mathcal{H}}\,.$$

Next, from the definition of $b_h(\cdot,\cdot)$ in (28), norm $\|\cdot\|_{\mathcal{H}}$ in (37), (40), (42), and the stability of T_h in (26), it holds

$$b_h(\bar\mu_H,v_0)\geq(1-\frac{\alpha\,C_b}{2})\,\|v_0\|_{\mathcal{H}}^2\geq C\,(1-\frac{\alpha\,C_b}{2})\,\|v_0\|_{\mathcal{H}}|\bar\mu_H|_\Lambda\,,$$

where C_b depends only on the Poincaré and trace constants. By choosing $\alpha\leq\frac{1}{C_b}$, we arrive at

$$\sup_{\mu_H\in\Lambda_H}\frac{b_h(\mu_H,v_0)}{|\mu_H|_\Lambda}\geq C\,\frac{1}{2}\,\|v_0\|_{\mathcal{H}}\,.\tag{58}$$

Then, using $\alpha\leq\min\left\{\frac{1}{C_b},\frac{1}{C_a}\right\}$, the (55), (56) and (58) also hold, which are the conditions for the existence and uniqueness of a solution for method (27) (see [23, Theorem 3.3.1]). In addition, the inf-sup condition (50) holds following closely the proof in [13, Proposition 2.36]. □
Error estimates for the discrete solution of (27) and its enriching counterpart (34) are next.

5 Error Analysis

This section presents *a priori* error estimates for the PGMHM method under the following assumption on the mesh skeleton:

Assumption A: The family of meshes $\{\mathcal{E}_H\}_{H>0}$ induces a shape regular family of triangulation $\{\Xi_H^K\}_{H>0}$ for each $K\in\mathscr{P}$, such that their trace on ∂K coincides with $\{\mathcal{E}_H\}_{H>0}$.

Notice that Assumption A yields a conforming simplicial partition $\Xi_H := \cup_{K\in}\Xi_H^K$ of Ω with the following property: for each $F \in \mathcal{E}_H$, there exists an element $T \in \Xi_H$ with face F.

Next, we recall some important estimates to measure the impact of the second-level discretization. Following [3, 14], we define $w_h := T_h\mu + \hat{T}_h f \in \tilde{V}_h(K)$ as the unique solution of the problem

$$\int_K A\nabla(T_h\mu + \hat{T}_h f)\cdot\nabla v_h \;= \langle\mu, v_h\rangle_{\partial K} + \int_K f\, v_h \;= \int_K A\nabla(T\mu + \hat{T} f)\cdot\nabla v_h\,,$$

for all $v_h \in \tilde{V}_h(K)$, and thus, using Cea's Lemma (c.f. [13, Lemma 2.28]), the following estimate follows

$$\|T\mu + \hat{T}f - w_h\|_{1,K} \le C_K \inf_{v_h\in\tilde{V}_h(K)} \|T\mu + \hat{T}f - v_h\|_{1,K}\,, \tag{59}$$

where C_K depends on the ratio of $A_{\max}$ and $A_{\min}$ in K, but is independent of h, H, or $\mathcal{H}$. Moreover, under the assumption that (13)-(14) have smoothing properties, in the sense of [13, Definition 3.14], and using [13, Theorem 3.18] we also get

$$\|T\mu + \hat{T}f - w_h\|_{0,K} \le C_K\, h \inf_{v_h\in\tilde{V}_h(K)} \|T\mu + \hat{T}f - v_h\|_{1,K}\,. \tag{60}$$

Before presenting the main error estimate, we recall the following approximation result concerning space Λ_H. A version of this result was originally presented in [15], and revised in [14] in the context of two-dimensional polytopal elements, and further extended to the tri-dimensional case in [22]. Here, we state the result proposed in [22] in the scalar functional case, for the sake of completeness (see [17, Lemma 5.1] for details).

Lemma 5.1. *Suppose Assumption A holds and let $w \in H^{m+1}(\mathscr{P})\cap H_0^1(\Omega)$ and $A\nabla w \in [H^m(\mathscr{P})]^d$, and $A\nabla w \in H(div,\Omega)$ with $1 \le m \le \ell+1$ and $\ell \ge 0$. Let $\mu \in \Lambda$ be such that $\mu|_E := A\nabla w\cdot \boldsymbol{n}^K\,|_E$ for each $E \in \mathcal{E}$. There exists a positive constant C, independent of h, H, $\mathcal{H}$ and A, such that*

$$\inf_{\mu_\ell\in\Lambda_H} \|\mu - \mu_\ell\|_\Lambda \le C\, H^m\, |A\nabla w|_{m,\mathscr{P}}\,, \tag{61}$$

where Λ_H is given in (23).

We are ready to present the main convergence result.

Theorem 5.2. *Let us assume that u, solution of (12) belongs to $H^{s+1}(\mathscr{P})$ and $A\nabla u \in [H^m(\mathscr{P})]^d$, with $1 \le s \le k$ and $1 \le m \le \ell+1$, $\ell \ge 0$ and $k \ge \ell + d$. Then, there exists C such that*

$$\|u_0 - u_0^h\|_V + |\lambda - \lambda_H|_\Lambda \le C\left(h^s\,|u|_{s+1,\mathscr{P}} + H^m\,|A\nabla u|_{m,\mathscr{P}}\right). \tag{62}$$

In addition, if $u_{Hh} := u_0^h + T_h\lambda_H + \hat{T}_h f$, then the following error estimate holds

$$\|u - u_{Hh}\|_V \le C\left(h^s\,|u|_{s+1,\mathscr{P}} + H^m\,|A\nabla u|_{m,\mathscr{P}}\right). \tag{63}$$

Proof. First observe that $\lambda \in L^2(\partial\mathscr{P})$, and let $\mu_H \in \Lambda_H$ be such that $\mu_H|_F$ is the $L^2(F)$ projection of λ on $\mathbb{P}_\ell(F)$, for all $F \in \mathcal{E}_H$ and $\ell \ge 0$. Note that $\lambda - \mu_H \in \mathscr{N}$. Then, from (50) and stability of T_h in (26) it holds

$$\begin{aligned}
&C\,|(\lambda_H - \mu_H, u_0 - u_0^h)|_{\Lambda\times\mathcal{H}}\\
&\quad\le \sup_{(\chi_H,w_0)\in\Lambda_H\times V_0} \frac{B_h(\lambda_H - \mu_H, u_0 - u_0^h; \chi_H, w_0)}{|(\chi_H,w_0)|_{\Lambda\times\mathcal{H}}}\\
&\quad\le \sup_{(\chi_H,w_0)\in\Lambda_H\times V_0} \frac{B_h(\lambda - \mu_H, 0; \chi_H, w_0)}{|(\chi_H,w_0)|_{\Lambda\times\mathcal{H}}}\\
&\qquad + \sup_{(\chi_H,w_0)\in\Lambda_H\times V_0} \frac{B_h(\lambda - \lambda_H, u_0 - u_0^h; \chi_H, w_0)}{|(\chi_H,w_0)|_{\Lambda\times\mathcal{H}}}\\
&\quad\le C\,\|\lambda - \mu_H\|_\Lambda + \sup_{(\chi_H,w_0)\in\Lambda_H\times V_0} \frac{B_h(\lambda - \lambda_H, u_0 - u_0^h; \chi_H, w_0)}{|(\chi_H,w_0)|_{\Lambda\times\mathcal{H}}}\,.
\end{aligned} \tag{64}$$

Next, we estimate the consistency error using (49) and (64), to arrive at

$$|(\lambda_H - \mu_H, u_0 - u_0^h)|_{\Lambda\times\mathcal{H}} \leq C \left(\|\lambda - \mu_H\|_\Lambda + \|(T - T_h)\lambda + (\hat{T} - \hat{T}_h)f\|_V \right) .$$

Then, using the fact that $u = u_0 + T\lambda + \hat{T}f \in H^{s+1}(K)$ and (59), it holds

$$\|T\lambda + \hat{T}f - \left(\hat{T}_h f + T_h\lambda\right)\|_V \leq C\, h^s\, |u|_{s+1,\mathscr{P}} , \tag{65}$$

which combined with Lemma 5.1 yields

$$|(\lambda_H - \mu_H, u_0 - u_0^h)|_{\Lambda\times\mathcal{H}} \leq C \left(h^s\, |u|_{s+1,\mathscr{P}} + H^m\, |A\nabla u|_{m,\mathscr{P}} \right) .$$

Estimate (62) follows from the triangle inequality and Lemma 5.1, which leads to

$$|(\lambda - \lambda_H, u_0 - u_0^h)|_{\Lambda\times\mathcal{H}} \leq C \left(h^s\, |u|_{s+1,\mathscr{P}} + H^m\, |A\nabla u|_{m,\mathscr{P}} \right) , \tag{66}$$

and then (62) follows using (40). Regarding (63), we perform as follows

$$\begin{aligned}
\|u - u_{Hh}\|_V &\leq \|u_0 - u_0^h\|_V + \|T\lambda + \hat{T}f - (T_h\lambda_H + \hat{T}_h f)\|_V \\
&\leq \|u_0 - u_0^h\|_V + \|T\lambda + \hat{T}f - (T_h\lambda + \hat{T}_h f)\|_V + \|T_h(\lambda_H - \lambda)\|_V \\
&\leq C \left(h^s\, |u|_{s+1,\mathscr{P}} + H^m\, |A\nabla u|_{m,\mathscr{P}} \right) ,
\end{aligned}$$

where we used the stability of T_h in (26), (65) and (62). □

5.1 An Error Estimate for $\|u - \tilde{u}_{Hh}\|_V$

The next result addresses the convergence of the discrete enriched solution $\tilde{u}_{Hh}$ given in (34).

Lemma 5.3. *Assume the hypothesis of Theorem 5.2 hold. Then, defining $\tilde{u}_{Hh} := u_0^h + T_h\tilde{\lambda}_H + \hat{T}_h f$, the following error estimate holds*

$$\|u - \tilde{u}_{Hh}\|_V \leq C \left(h^s\, |u|_{s+1,\mathscr{P}} + H^m\, |A\nabla u|_{m,\mathscr{P}} \right) . \tag{67}$$

Proof. First, let $E \in \mathcal{E}_0$ be a face and $K, K' \in \mathscr{P}$ the two elements sharing E. Select $\mu_H^\star \in \Lambda_H$ as $\mu_H^\star|_{E\cap\partial K} := [\![u_0 - u_0^h]\!]\,|_E$ and $\mu_H^\star|_{E\cap\partial K'} := -[\![u_0 - u_0^h]\!]\,|_E$, and zero elsewhere. If $E \in \mathcal{E} \cap \partial\Omega$, then take $\mu_H^\star|_{E\cap\partial K} := (u_0 - u_0^h)\,|_E$ where K is the element containing E. Then, testing (36) and (16) with $(\mu_H^\star, 0)$, and following closely the proof of [17, Theorem 5.4], we get

$$\Big(\sum_{E\in\mathcal{E}} \frac{1}{\mathcal{H}_E} \|\left[\!\left[u_0 - u_0^h\right]\!\right]\|_{0,E}^2 \Big)^{1/2} \leq C\, \|\nabla(u - u_{Hh})\|_{0,\mathscr{P}} . \tag{68}$$

From the definition of λ_R in (32), the regularity of u, and the trace inequality in (42) and (68), it holds

$$\begin{aligned}
\sum_{E\in\mathcal{E}} \mathcal{H}_E \|\lambda_R\|_{0,E}^2 &\leq C \Big(\sum_{E\in\mathcal{E}_0} \frac{1}{\mathcal{H}_E} \|[\![u_{Hh}]\!]\|_{0,E}^2 + \sum_{E\subset\partial\Omega} \frac{1}{\mathcal{H}_E} \|\pi_k\, g - u_{Hh}\|_{0,E}^2 \Big) \\
&\leq C \sum_{E\in\mathcal{E}} \frac{1}{\mathcal{H}_E} \|[\![u - u_{Hh}]\!]\|_{0,E}^2 \\
&\leq C \Big[\sum_{E\in\mathcal{E}} \frac{1}{\mathcal{H}_E} \|\left[\!\left[u_0 - u_0^h\right]\!\right]\|_{0,E}^2 \\
&\qquad + \sum_{E\in\mathcal{E}} \frac{1}{\mathcal{H}_E} \|[\![T\lambda + Tf - T_h\lambda_H - T_h f]\!]\|_{0,E}^2 \Big] \\
&\leq C\, \|\nabla(u - u_{Hh})\|_{0,\mathscr{P}}^2 \\
&\leq C \left(h^{2s}\, |u|_{s+1,\mathscr{P}}^2 + H^{2m}\, |A\nabla u|_{m,\mathscr{P}}^2 \right) ,
\end{aligned} \tag{69}$$

where we used Theorem 5.2 in the last step.

Next, we estimate $u_R := T_h\lambda_R \in \tilde{V}_h$. For that, we use inequality (42), (33) and (2), Cauchy-Schwartz inequality and the definition of norm $\|\cdot\|_{\mathcal{H}}$ as follows

$$\begin{aligned}
\|u_R\|_{\mathcal{H}}^2 &\leq C \sum_{K\in\mathscr{P}} \|\nabla T_h\lambda_R\|_{0,K}^2 \\
&\leq C \sum_{K\in\mathscr{P}} \langle \lambda_R, T_h\lambda_R\rangle_{\partial K} \\
&\leq C \sum_{E\in\mathcal{E}} \|\lambda_R\|_{0,E} \|[\![T_h\lambda_R]\!]\|_{0,E} \\
&\leq C \Big[\sum_{E\in\mathcal{E}} \mathcal{H}_E \|\lambda_R\|_{0,E}^2\Big]^{1/2} \Big[\sum_{E\in\mathcal{E}} \frac{1}{\mathcal{H}_E} \|[\![T_h\lambda_R]\!]\|_{0,E}^2\Big]^{1/2} \\
&\leq C \Big(\sum_{E\in\mathcal{E}} \mathcal{H}_E \|\lambda_R\|_{0,E}^2\Big)^{1/2} \|u_R\|_{\mathcal{H}}\,,
\end{aligned} \tag{70}$$

and as result, we get

$$\|u_R\|_{\mathcal{H}} \;\leq\; C \Big(\sum_{E\in\mathcal{E}} \mathcal{H}_E \|\lambda_R\|_{0,E}^2\Big)^{1/2}.$$

Then, using (40) and (69), we arrive at

$$\|u_R\|_V \;\leq\; C\,\|u_R\|_{\mathcal{H}} \;\leq\; C\left(h^s\,|u|_{s+1,\mathscr{P}} + H^m\,|A\nabla u|_{m,\mathscr{P}}\right). \tag{71}$$

The result (67) follows from the definition of $\tilde{u}_{Hh}$ in (34) and the triangle inequality

$$\|u - \tilde{u}_{Hh}\|_V \leq \|u - u_{Hh}\|_V + \|u_R\|_V\,,$$

and using (71) and Theorem 5.2.

□

6 Numerical validation

This section verifies the theoretical aspects of the method (27). The goal of the first experiment is to assess the theoretical results using a smooth analytical solution, while the second and third test cases aim at showing the robustness of the method when applied to problems with highly heterogeneous coefficients. We shall distinguish two kinds of convergences, namely,

- $\mathcal{H} \to 0$ called the mesh-based convergence;
- $H \to 0$ with $\mathcal{H}$ fixed called the space-based convergence.

Second-level meshes are made of triangles that respect the requirement for the well-posedness of the PGMHM method, i.e., $k \geq \ell + 2$. Their diameter h tends to zero in both mesh-based and space-based convergence validations.

Following [17], the convergence history is measured in the $L^2(\Omega)-$ and $H^1(\mathscr{P})-$norms for the primal variable u_{Hh}, and in the following $H(\mathrm{div}, \mathscr{T}_h)-$norm

$$\|\boldsymbol{\sigma}\|_{\mathrm{div}} := \left(\sum_{K\in\mathscr{P}} \sum_{T\in\mathscr{T}_h^K} \|\boldsymbol{\sigma}\|_{0,T}^2 + h_{\partial\Omega}^2 \|\nabla\cdot\boldsymbol{\sigma}\|_{0,T}^2\right)^{1/2},$$

for the post-processed stress tensor $\boldsymbol{\sigma}_{Hh} := A\,\nabla\tilde{u}_{Hh}$.

6.1 An analytical solution case

We consider an analytical solution

$$u(x, y) = \sin(2\pi x)\sin(2\pi y)$$

on a unit square and prescribe the corresponding homogeneous Dirichlet boundary conditions and right-hand side, with A being the identity matrix. We use global meshes based on triangles and on L-shaped elements.

For the mesh-based convergence, we use $H = \mathcal{H}$, that means that we do not divide the edges of the partitions any further. The results for the two types of meshes cited above with $\ell \in \{0, 1\}$ can be seen in Figure 3 and Figure 4, respectively. We illustrate in Figure 2 two L-shaped global meshes with their overlaid solutions.

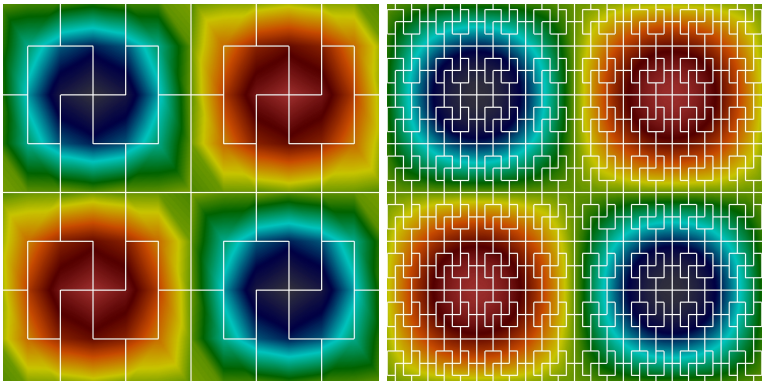

Figure 2: Isolines of the numerical solutions on L-shaped meshes.

We remark that all the errors tend to zero as predicted by theory in Section 5. Interestingly, for the case $\ell = 0$ on simplicial meshes the norm $\|\boldsymbol{\sigma}_{Hh} - A\nabla u\|_{\text{div}}$ shows $\mathcal{O}(H^{\ell})$ convergence, while this does not occur for the L-shaped mesh (See Figures 3 and 4). Such experiments used one-element second level meshes with a polynomial degree of order $k = \ell + 2$ for the simplicial element case.

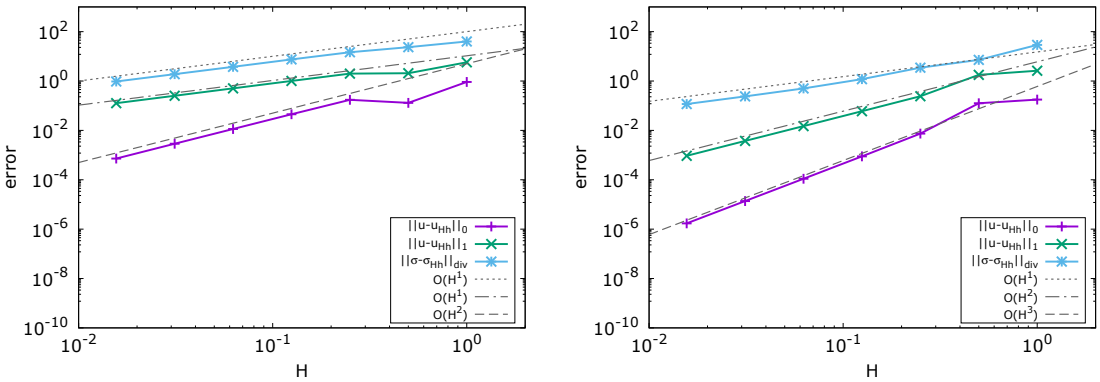

Figure 3: The mesh-based convergence on simplicial elements for $\ell = 0$ (left) and $\ell = 1$ (right).

Next, we report the results obtained for the space-based strategy. For this, we fixed the coarse mesh with 16 triangular elements or 32 L-shaped elements. The edges get refined as well as the second level sub-meshes. It's interesting to notice that for $\ell = 1$ we obtain an unexpected extra order of convergence $\mathcal{O}(H^{1/2})$, while for $\ell = 0$ case an additional $\mathcal{O}(H)$ order of the convergence were found. These very attractive features deserve more investigation, and can be seen in Figures 5 and 6. An additional $\mathcal{O}(H^{1/2})$ rate of convergence was also observed in the original MHM method and theoretically investigated in [24].

We also compare the solutions from the mesh-based and the space-based using $\ell \in \{0, 1\}$ in the L^2 and H^1 norms with respect to the number of degrees of freedom. Figure 7 shows the case of triangular L-

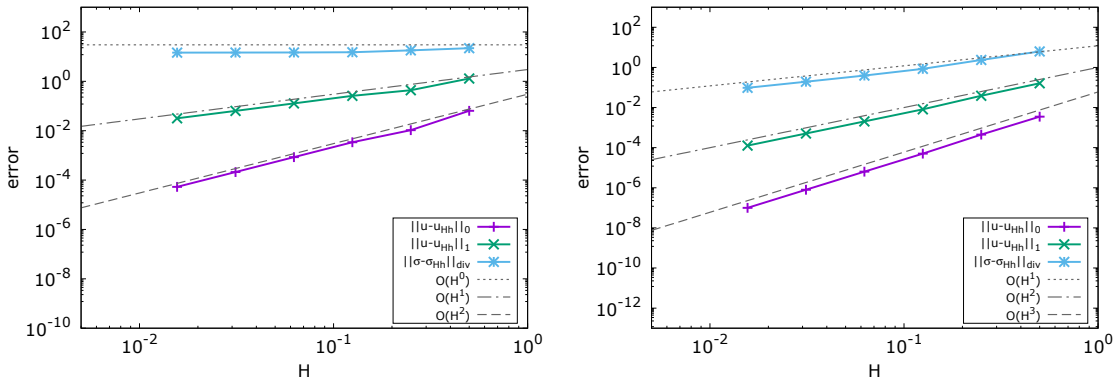

Figure 4: The mesh-based convergence history on L-shaped elements for $\ell = 0$ (left) and $\ell = 1$ (right).

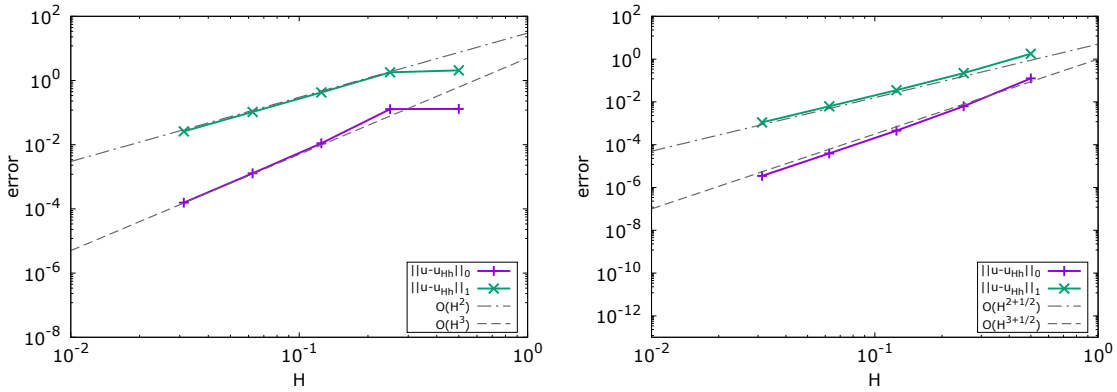

Figure 5: The spaced-based convergence on simplicial elements for $\ell = 0$ (left) and $\ell = 1$ (right).

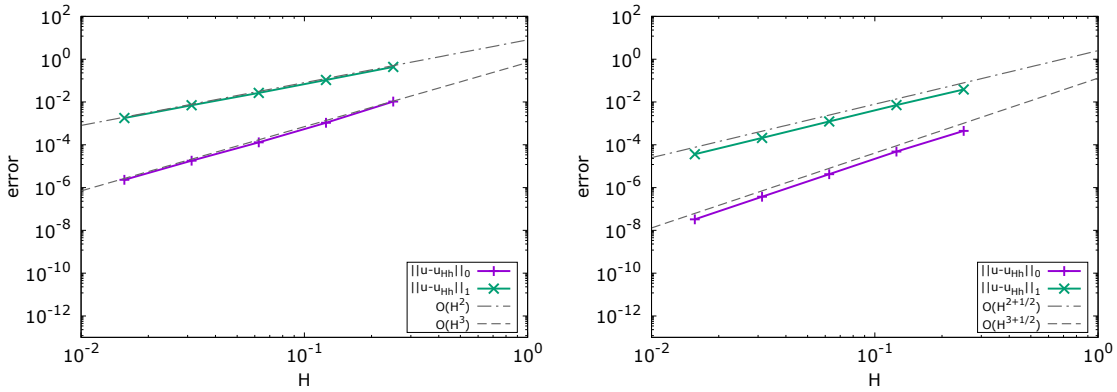

Figure 6: The spaced-based convergence on L-shaped elements for $\ell = 0$ (left) and $\ell = 1$ (right).

shaped element meshes. We can see that the space-based case requires fewer degrees of freedom compared to the mesh-based strategy to achieve a certain error threshold.

6.2 A heterogeneous media case

The domain corresponds to a unit square with 27×27 square inclusions in which the diffusion coefficient has different values as proposed in [14]. The domain setting is depicted in Figure 8 for the case with three inclusions in each direction. The diffusion matrix is given by $A = \kappa I$ with $\kappa = 1$ in the blue region

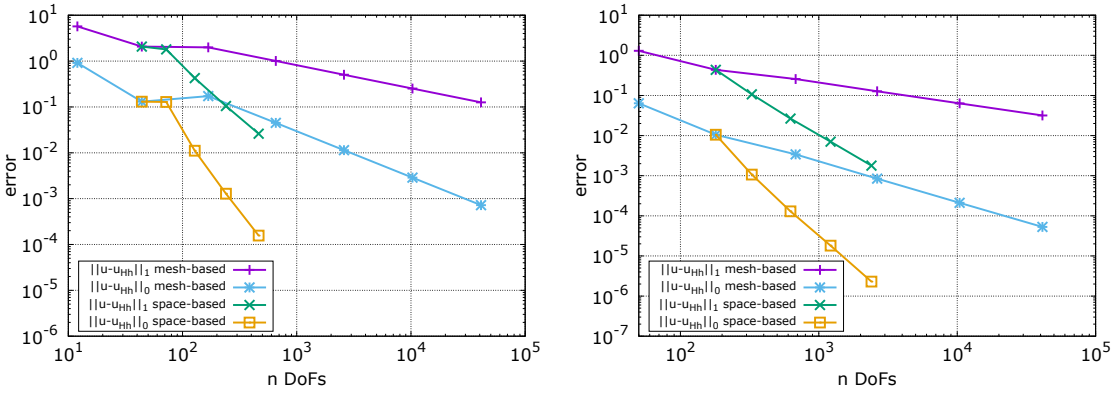

Figure 7: Comparision between mesh-based and space-based convergences on simplicial elements (left) and L-shaped elements (right) in the L^2 and H^1 norms with respect to the DoF. Here $\ell = 0$.

and $\kappa = 10^5$ in the green one, where I stands for the identity matrix. The boundary conditions are homogeneous Dirichlet in the whole boundary and $f = 1$ in Ω.

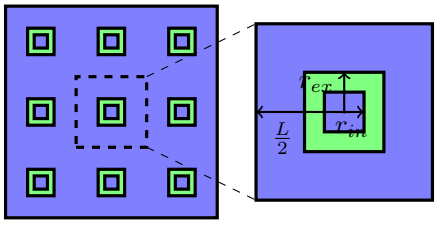

Figure 8: A sketch of a heterogeneous diffusive media. Here $r_{in} = \frac{1}{32}$, $r_{ex} = \frac{1}{16}$, $L = \frac{1}{4}$. Coefficient's values are $\kappa = 1$ (blue) and $\kappa = 10^5$ (green).

We compute a reference solution using a refined global mesh with over 100,000 triangular elements using the MHM method with constant interpolation on faces (see Figure 9).

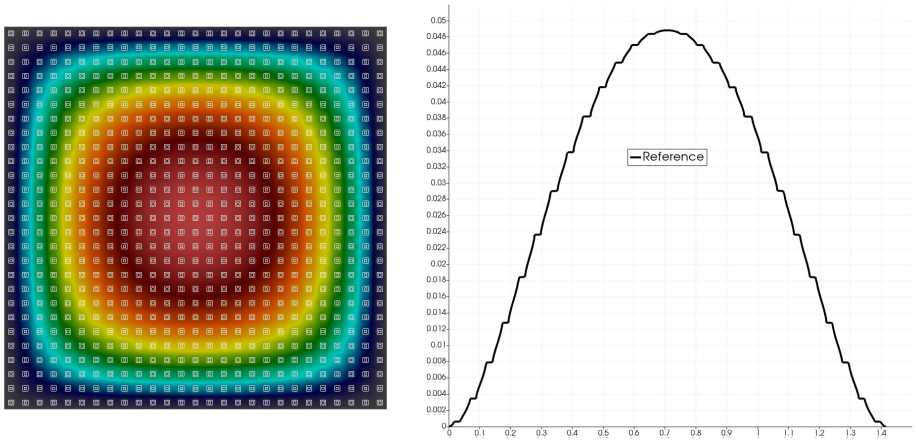

Figure 9: The 27×27 inclusion teste case: Reference solution on a triangular mesh with DoF= 328,192 using the MHM method with $\ell = 0$. The right figure shows the profile solution at $y = x$.

We solve the model using a L-shaped mesh with 328 degrees. Observe that the PGMHM method provides a more accurate solution than the one from the MHM method (see Figure 10). It indicates that

the additional terms in the PGMHM method may play an important role in heterogeneous cases. Such a difference decreases as the mesh get refined as expected.

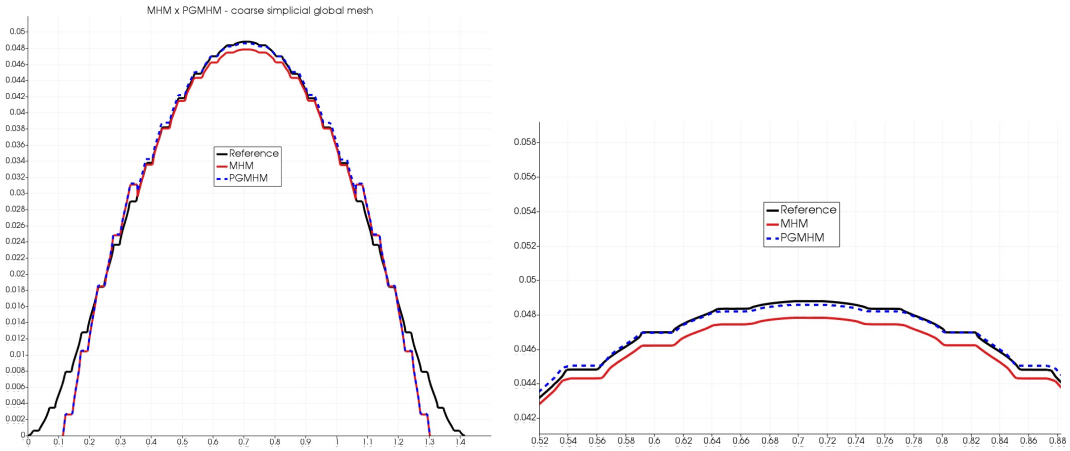

Figure 10: The 27×27 inclusion teste case: Comparison of the solutions using the MHM and PGMHM method on a simplicial coarse global mesh. Here $\ell = 0$.

6.3 SPE 10

We use the Model 2 of the 10th Society of Petroleum Engineers Comparative Solution Project (cf. [25]) hereafter referred to as the SPE-10 model. As detailed in [26], the model represents a very heterogeneous reservoir and is represented by a regular Cartesian grid. The model dimensions are $1200 \times 2200 \times 170$(ft). It consists of part of a Brent sequence, with top 70 ft (35 layers) represents the Tarbert formation, which is a representation of a prograding nearshore environment and the bottom 100 ft (50 layers) represents Upper Ness, which is fluvial. The fine-scale (geological) model contains $60 \times 220 \times 85$ blocks or cells (for a total of 1,122,000 cells), with the block size at the fine-scale being $20 \times 10 \times 2$(ft).

To validate our method using the model described above, we are going to choose the first layer as the object of our study and set the entry pressures as $u = 1$ (bottom side) and exit $u = 0$ (upper side). On the other two boundaries, we set the homogeneous Neumann condition. Notice that Neumann boundary conditions can be handle in the PGMHM method as in the MHM method., i.e. as an essencial condition (see [17, Remark 2.3] for details).

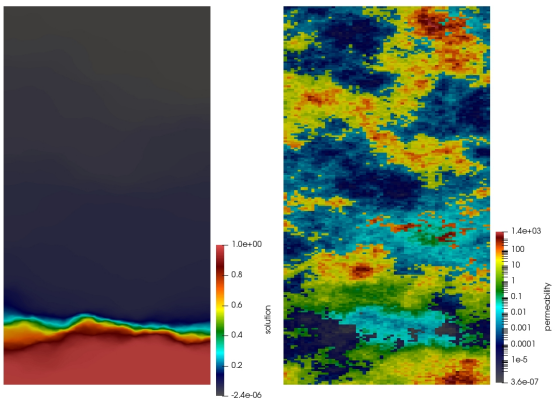

Figure 11: Reference solution (left) on the first layer for the SPE10 case (right).

For the reference solution (see Figure 11), we used a quadrilateral mesh with $DoF = 118,160$ and

over 2,000,000 elements. According to the theory proved in Section 5, as we refine the global mesh the numerical solution should get closer to the reference. We observe such a behavior in Figure 12 (right).

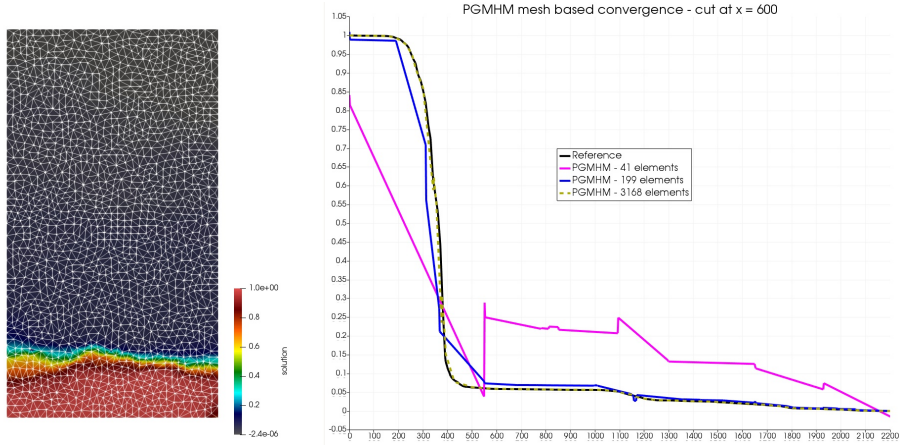

Figure 12: A study of a mesh-based convergence on three different unstructured triangular meshes, $\ell = 0$.

Next, we set a coarse global mesh with only two elements and refine the second level meshes (see Figure 13). We used 2048 elements in total. We can observe that, as we refine the edges (space-based approach), the solution gets closer to the reference solution and with a number of mesh degrees of freedom far lower than the one in the reference. In fact, the best approximation has only 14 degrees of freedom.

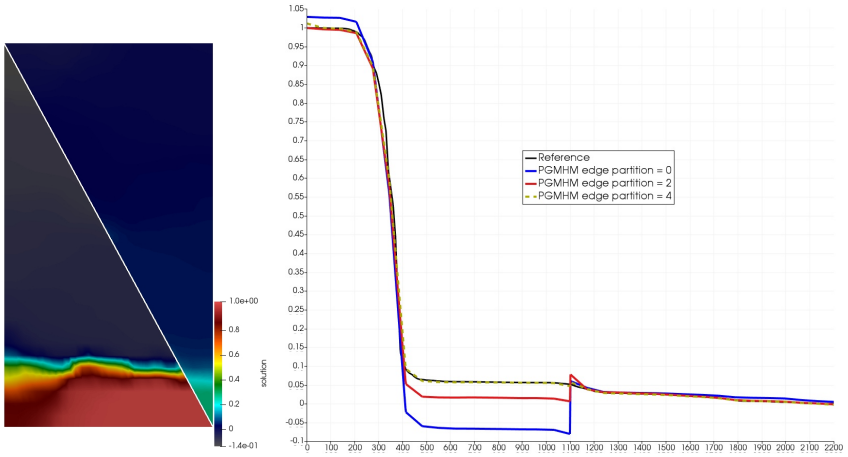

Figure 13: Solution using a global mesh with only two elements with the overlaid solution (left) and a study of convergence of the space-based approach (right). Here the sub-meshes are very refined and contain 2,048 elements. Here $\ell = 0$.

We conclude that the space-based strategy appears as the better option to handle highly heterogeneous media problems with respect to the number of degree of freedom needed to achieve a target accuracy.

7 Conclusions

In this work, we proposed, analyzed, and validated a new multiscale finite element method, called PGMHM method, for the two- and three-dimensional Darcy problem. The method emerged from the enrichment of the Lagrange multiplier trial space, which after a static condensation procedure, turns out to be a way to enforce the H^1-conformity of the MHM method. Also, it yields a natural way to post-process the numerical solution through a "physical" Lagrange multiplier space which may help dealing with highly heterogeneous media.

From the theoretical viewpoint, we proved the well-posedness of the PGMHM method by showing the continuity and an inf-sup condition for the (bi)linear forms associated with the PGMHM method. Next, we showed that the method delivers an optimally-convergent numerical solution in the broken H^1-norm. We also extended such an analysis to the post-processed numerical solution.

The numerical results support the theoretical results. Also, interestingly, we found (numerically) unexpected extra orders of convergences in the case of the space-based approach (and also for the norm $\|\cdot\|_{\text{div}}$ in the mesh-based approach for $\ell = 0$ on a triangular mesh). Indeed, numerics pointed out additional $\mathcal{O}(H^{1/2})$ and $\mathcal{O}(H)$ rates of convergence whether ℓ is odd or even, respectively, in the space-based convergence case. Such results are also present in the MHM method, which shows an additional $\mathcal{O}(H^{1/2})$. In the case of even ℓ, the super-convergence is new and deserves theoretical investigations. Numerical results for the heterogeneous problems also confirmed that the space-based strategy is better than the mesh-based one as long as the number of degrees of freedom is concerned with achieving a given error threshold.

Regarding numerical differences between the MHM and the PGMHM methods, we found that the PGMHM method yielded slightly more accurate solutions than the MHM method on a heterogeneous media case. In addition, further investigation is needed, mainly for measuring the impact of the post-processing strategy on the numerical solution's accuracy, an aspect of the PGMHM method not explored computationally in the present work.

Funding The second author was funded by Coordenação de Aperfeiçoamento de Pessoal de Nível Superior (CAPES). The fourth author was partially supported by CNPq/Brazil No. 309173/2020-5 and FAPERJ E-26/201.182.2021, and by Inria/France under the Inria International Chair.

Acknowledgments The authors acknowledge the IPES research group (http://ipes.lncc.br/) for its support, and the National Laboratory for Scientific Computing (LNCC/MCTI, Brazil) for providing HPC resources of the SDumont supercomputer (http://sdumont.lncc.br).

References

[1] I. Babuska and E. Osborn. "Generalized finite element methods: Their performance and their relation to mixed methods". In: *SIAM J. Num. Anal.* 20.3 (1983), pp. 510–536.

[2] C. Harder, D. Paredes, and F. Valentin. "A family of Multiscale Hybrid-Mixed finite element methods for the Darcy equation with rough coefficients". In: *J. Comput. Phys.* 245 (2013), pp. 107–130.

[3] R. Araya, C. Harder, D. Paredes, and F. Valentin. "Multiscale Hybrid-Mixed Method". In: *SIAM J. Numer. Anal.* 51.6 (2013), pp. 3505–3531.

[4] T. JR Hughes, G. R Feijó, L. Mazzei, and J.B. Quincy. "The variational multiscale method—a paradigm for computational mechanics". In: *Computer methods in applied mechanics and engineering* 166.1-2 (1998), pp. 3–24.

[5] Y.R. Efendiev, T.Y. Hou, and X.H. Wu. "Convergence of a nonconforming multiscale finite element method". In: *SIAM J. Numer. Anal.* 37.3 (2000), 888–910 (electronic).

[6] H. Fernando, C. Harder, D. Paredes, and F. Valentin. "Numerical multiscale methods for a reaction-dominated model". In: *Computer Methods in Applied Mechanics and Engineering* 201 (2012), pp. 228–244.

[7] A. Abdulle, E Weinan, B. Engquist, and E. Vanden-Eijnden. "The heterogeneous multiscale methods". In: *Communications in Mathematical Sciences* 1.1 (2003), pp. 87–132.

[8] T. Arbogast, G. Pencheva, M. F. Wheeler, and I. Yotov. "A multiscale mortar mixed finite element method". In: *SIAM Multiscale Modeling and Simulation* 6 (2007), pp. 319–346.

[9] A. Malqvist and D. Peterseim. "Localization of Elliptic Multiscale Problems". In: *Math. Comp.* 83.290 (2014), pp. 2583–2603.

[10] O. Duran, P. R. B Devloo, S. M. Gomes, and F. Valentin. "A multiscale hybrid method for Darcy's problems using mixed finite element local solvers". In: *Comp. Meth. Appl. Mech. Eng.* 354 (2019), pp. 213–244.

[11] R. Araya, G. R. Barrenechea, L. P. Franca, and F. Valentin. "Stabilization arising from PGEM: A review and further developments". In: *Applied Numerical Mathematics* 59.9 (2009), pp. 2065–2081.

[12] C. Harder, D. Paredes, and F. Valentin. "On a multiscale hybrid-mixed method for advective-reactive dominated problems with heterogeneous coefficients". In: *Multiscale Modeling & Simulation* 13.2 (2015), pp. 491–518.

[13] Alexandre Ern and Jean-Luc Guermond. *Theory and Practice of Finite Elements*. 1st ed. New York, NY: Springer, 2004.

[14] G.R. Barrenechea, F. Jaillet, D. Paredes, and F. Valentin. "The multiscale hybrid mixed method in general polygonal meshes". In: *Numer. Math.* 145 (2020), pp. 197–237.

[15] P.A. Raviart and J.M. Thomas. "Primal Hybrid Finite Element Methods for 2nd Order Elliptic Equations". In: *Math. Comp.* 31.138 (1977), pp. 391–413.

[16] C. Harder and F. Valentin. "Foundations of the MHM method". In: *Building Bridges: Connections and Challenges in Modern Approaches to Numerical Partial Differential Equations*. Ed. by G. R. Barrenechea, F. Brezzi, A. Cangiani, and E. H. Georgoulis. Lecture Notes in Computational Science and Engineering. Edinburgh: Springer, 2016.

[17] A. T. A. Gomes, W. Pereira, and F. Valentin. "The MHM Method for Linear Elasticity on Polytopal Meshes". In: *to appear in IMA Journal of Numerical Analysis* (2022).

[18] G. R. Barrenechea and F. Valentin. "Consistent local projection stabilized finite element methods". In: *SIAM J. Numer. Anal.* 48.5 (2010), pp. 1801–1825.

[19] L. Beirão da Veiga, C. Lovadina, and A. Russo. "Stability analysis for the virtual element method". In: *Mathematical Models and Methods in Applied Sciences* 27.13 (2017), pp. 2557–2594.

[20] L. E Payne and H. F. Weinberger. "An optimal Poincaré inequality for convex domains". In: *Archive for Rational Mechanics and Analysis* 5.1 (1960), pp. 286–292.

[21] A. Veeser and R. Verfürth. "Poincaré constants for finite element stars". In: *IMA Journal of Numerical Analysis* 32.1 (2011), pp. 30–47.

[22] W. Pereira. "Multiscale Hybrid-Mixed Methods for Elastic Models in Heterogeneous Media". PhD thesis. Ph. D. thesis, National Laboratory for Scientific Computing (LNCC), Rio de Janeiro, Brasil, 2019.

[23] Daniele Boffi, Franco Brezzi, Michel Fortin, et al. *Mixed finite element methods and applications*. 1st ed. Berlin, Heidelberg: Springer, 2013.

[24] T. Chaumont-Frelet, D. Paredes, and F. Valentin. "Flux Approximation on Unfitted Meshes and Application to Multiscale Hybrid-Mixed Methods," in preparation.

[25] M. A. Christie and M. J Blunt. "Tenth SPE comparative solution project: A comparison of upscaling techniques". In: *SPE Reservoir Simulation Symposium*. Society of Petroleum Engineers. 2001.

[26] M. R. Rasaei and M. Sahimi. "Upscaling and simulation of waterflooding in heterogeneous reservoirs using wavelet transformations: application to the SPE-10 model". In: *Transport in Porous Media* 72.3 (2008), pp. 311–338.